Water Oxidation

DOI: 10.1002/anie.201004278

Chemical and Light-Driven Oxidation of Water Catalyzed by an Efficient Dinuclear Ruthenium Complex**

*Yunhua Xu, Andreas Fischer, Lele Duan, Lianpeng Tong, Erik Gabrielsson, Björn Åkermark, and Licheng Sun**

Photoinduced water splitting that converts solar energy into molecular hydrogen is one of the most promising ways for producing a clean fuel that can meet the future need for environmentally friendly and renewable energy sources.[1] Oxidation of water into molecular oxygen is the key challenge in the construction of a system that is able to induce water splitting. An efficient and practical catalyst for water oxidation should show a high turnover number (TN), which reflects high stability, a high turnover frequency (TOF), which reflects high activity, and a low overpotential. Much effort has been spent on the development of efficient molecular catalysts for homogeneous water oxidation, which include complexes of Mn,[2–4] Ru,[2–17] and other metals.[3,4,18–20] Although some of these catalysts have shown promising activity, their efficiencies are still not high. The TN values are usually less than 3000 and the TOF values are less than $0.2\,s^{-1}$ when $Ce(NH_4)_2(NO_3)_6$ (Ce^{IV}) is used as the oxidant.[3,6c] Moreover, among these catalysts, only very few showed overpotentials that were low enough to permit homogeneous water oxidation driven by visible light when using $[Ru(bpy)_3]^{2+}$ ($E[Ru^{3+/2+}] = 1.26$ V vs. NHE; bpy = 2,2′-bipyridine) as the sensitizer.[11,14,16,17a]

Inspired by the oxygen-evolving complex in Photosystem II that contains oxygen-rich ligands, we employed carboxylate ligands to synthesize ruthenium-based complexes that can efficiently catalyze water oxidation.[10–13] Our previously reported dinuclear ruthenium complex (**A**), which has a *trans* structure,[12] gave a low TN value,[12a] and the overpotential was not low enough to allow photogenerated $[Ru(bpy)_3]^{3+}$ to drive **A** to catalyze water oxidation.[12b] To improve the performance of our catalysts, a new dinuclear ruthenium complex (**1**), which has a *cis* structure, has been designed and synthesized with ligand H_2L1 (H_2L1 = 1,4-bis(6′-COOH-pyrid-2′-yl)phthalazine). Herein, we report that complex **1** is indeed a very stable and efficient catalyst for both chemical and light-driven water oxidation, in fact far superior to complex **A** and other catalysts.

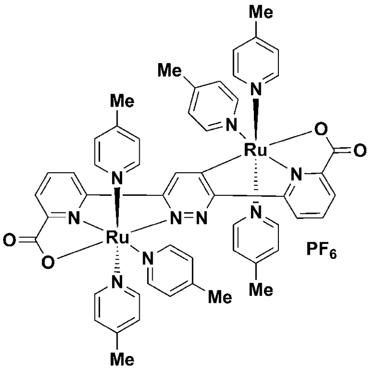

A

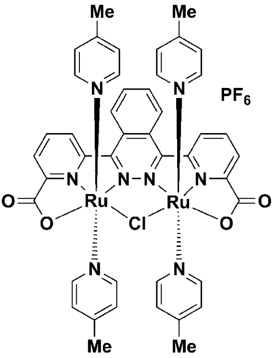

1

Ligand H_2L1 and complex **1** were synthesized (see Scheme S1 in the Supporting Information) by starting with the Stille cross-coupling of 2-tributylstannyl-6-methylpyridine and 1,4-dichlorophthalazine, to give 1,4-bis(6′-methylpyrid-2′-yl)phthalazine. Oxidation of the methyl groups with $Na_2Cr_2O_7$ in concentrated H_2SO_4 afforded ligand H_2L1. The 4,5 substitution in the pyridazine moiety contained in H_2L1 blocked the formation of the *trans* product. Therefore the desired *cis*-complex **1** was obtained in a moderate yield by reaction of H_2L1 with $[Ru(dmso)_4Cl_2]$ and subsequent treatment with 4-picoline (dmso = dimethyl sulfoxide). The structure of complex **1** was determined by NMR spectroscopy (see Figure S1 in the Supporting Information) and single-crystal X-ray analysis (see Figure S2 in the Supporting Information).[21] This diamagnetic $Ru_2^{II,II}$ complex has a symmetric structure with a μ-Cl bridge, and contains one negatively charged ligand $L1^{2-}$ and four picoline ligands. The high-resolution mass spectrum shows a corresponding monocharged $[\mathbf{1}\text{-}PF_6^{-}]^+$ signal at *m/z* 981.0757 (calcd *m/z* 981.0786), which further confirms the structure assignment. The bite angles of O-Ru-Cl are 100.6° and 100.7°, respectively, and are larger than the ideal value of 90° for an octahedral configuration. Interestingly, in the solid state, one water molecule is present between two molecules of **1**, and is hydrogen bonded to the adjacent

---

[*] Dr. Y. Xu, Dr. A. Fischer, L. Duan, L. Tong, E. Gabrielsson, Prof. L. Sun
Department of Chemistry
School of Chemical Science and Engineering
Royal Institute of Technology (KTH), 10044 Stockholm (Sweden)
Fax: (+46) 8-791-2333
E-mail: lichengs@kth.se
Prof. B. Åkermark
Department of Organic Chemistry, Arrhenius Laboratory
Stockholm University
10691 Stockholm (Sweden)
Prof. L. Sun
State Key Laboratory of Fine Chemicals, DUT-KTH Joint Education and Research Center on Molecular Devices, Dalian University of Technology (DUT)
Dalian 116012 (China)

[**] This work was supported by the Swedish Research Council, the K & A Wallenberg Foundation, the Swedish Energy Agency, and the China Scholarship Council. We thank Bao-Lin Lee at Stockholm University for high-resolution mass spectrometry measurements.

Supporting information for this article (experimental procedures) is available on the WWW under http://dx.doi.org/10.1002/anie.201004278.

oxygen atoms in the carbonyl groups of the carboxylate ligands. The complexes are thus connected through O-H···O bonds (see Figure S3 in the Supporting Information), thereby yielding infinite chains along the *a* axis.

The electrochemistry of complex **1** was investigated by cyclic voltammetry (CV) in both organic and aqueous solutions. The CV of **1** in dry acetonitrile (see Figure S4 in the Supporting Information) shows two reversible oxidation waves with a half-wave potential ($E_{1/2}$) values of 0.903 V and 1.396 V versus the normal hydrogen electrode (NHE). These two waves are assigned to the oxidation processes of $Ru_2^{II,II}$ to $Ru_2^{II,III}$, and $Ru_2^{II,III}$ to $Ru_2^{III,III}$, respectively. By introduction of the negatively charged ligand ($L1^{2-}$), the corresponding oxidation potentials of **1** are much lower than those of reported similar complexes with neutral ligands.[7a,b] However, the oxidation potentials are higher than those of complex **A** (see also Figure S4 in the Supporting Information), which has even lower oxidation potentials because of the strong electron-donating aryl group (carbon–ruthenium bond).[12a] In an aqueous solution with pH 1.0, complex **1** exhibits a pronounced electrocatalytic wave for water oxidation at potential values larger than 1.5 V versus NHE (see Figure S5a in the Supporting Information). At pH 7.2, this catalytic current has a much lower onset potential (ca. 1.20 V; see Figure S5b in the Supporting Information). The CV spectrum of **A** at pH 7.2 shows a catalytic water oxidation current with an onset potential at approximately 1.35 V.[12b]

Subsequently, the catalytic activity of **1** toward water oxidation was first investigated by using Ce^{IV} as the oxidant at pH 1.0. The oxygen that evolved in the headspace of the reaction flask was measured by gas chromatography (GC) and the reaction kinetics was monitored with an oxygen sensor. When a solution of **1** in acetonitrile was injected into an aqueous solution of Ce^{IV} at pH 1.0 (adjusted with CF_3SO_3H), rapid oxygen evolution was observed. At a high concentration of Ce^{IV} (330 mM), a TN value of 3540 for complex **1** was obtained. To date, this TN value is the highest one reported for the homogeneous system when Ce^{IV} is used as an oxidant.[3,6c] Under the same conditions, complex **A** gave a much lower TN value of 1690.

Interestingly, the catalytic activities of **1** and **A** were found to depend on the concentration of Ce^{IV}. Figure 1a shows the kinetics of oxygen evolution catalyzed by **1** (2 nmol) in the reaction mixture containing excess Ce^{IV} (5 mM). Under these conditions, approximately 20.7 μmol of O_2 was produced after a reaction time of 20 hours, thus giving an extremely high TN (ca. 10400). This record TN value is approximately ten times higher than the highest value reported for ruthenium-based catalysts and is four times higher than the highest value reported for iridium-based catalysts,[3,6c] thereby showing that complex **1** is the most stable water oxidation catalyst so far reported. Under the same conditions, complex **A** gave a TN of approximately 4700 (Figure 1b), and Ce^{IV} itself showed a negligible background for water oxidation (Figure 1c). The turnover numbers of catalysts **1** and **A** at various concentrations of Ce^{IV} are given in Table S1 of the Supporting Information. It is obvious that at low concentrations of Ce^{IV}, both complexes **1** and **A** have high TN values. The reason for this phenomenon is unclear, most likely it arises from the decomposition of the catalyst by ligand oxidation at high Ce^{IV} concentrations. We are currently investigating this aspect in more detail.

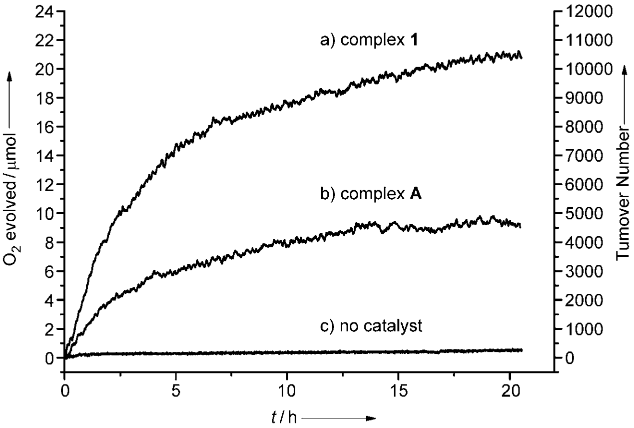

Figure 1. Kinetics of oxygen evolution by Ce^{IV} (5 mM) in an aqueous CF_3SO_3H solution (pH 1.0, 40 mL) in the presence of a) **1** (0.05 μM), b) **A** (0.05 μM), and c) in the absence of the catalyst. The curves were measured by an O_2 sensor and calibrated by GC analysis.

The rate of oxygen evolution was found to follow first-order kinetics with respect to the catalyst concentration at low Ce^{IV} concentrations. The kinetics of oxygen evolution at various concentrations of **1** at $[Ce^{IV}] = 20$ mM are shown in Figure S6a of the Supporting Information, and the initial rates of oxygen formation showed a linear dependence of the catalyst concentrations (see Figure S6b in the Supporting Information). Under these conditions, a TOF value of 1.2 s^{-1} was achieved by **1**, while only a value of 0.28 s^{-1} was obtained for **A**. This TOF value for **1** is more than ten times higher than those found for ruthenium-based catalysts reported by other research groups.[3] In this regard, complex **1** is the most active catalyst to date.

It can be seen from the CV of **1** at pH 7.2 (Figure S5b in the Supporting Information) that the onset potential for catalytic water oxidation is lower than the oxidation potential of $[Ru(bpy)_3]^{3+}$, thereby indicating that this reaction could be driven by photogenerated $[Ru(bpy)_3]^{3+}$. To evaluate this possibility, an artificial system (Scheme S2 in the Supporting Information) containing the sacrificial electron acceptor persulfate ($S_2O_8^{2-}$),[14,16,17a,22] the sensitizer $[Ru(bpy)_3]^{2+}$ (**P1**, see the Supporting Information) and the catalyst **1** was used for light-driven water oxidation under neutral conditions [Eqs. (1) and (2)].

$$4[RuL_3]^{2+} + 2S_2O_8^{2-} \xrightarrow{h\nu} 4[RuL_3]^{3+} + 4SO_4^{2-} \tag{1}$$

$$4[RuL_3]^{3+} + 2H_2O \xrightarrow{1} 4[RuL_3]^{2+} + O_2 + 4H^+ \tag{2}$$

Figure 2a displays the kinetics of oxygen evolution measured by a Clark-type oxygen electrode from a phosphate buffer solution with a pH value of 7.2 and containing **1**, $[Ru(bpy)_3]^{2+}$, and $Na_2S_2O_8$ under irradiation with $\lambda > 400$ nm. Molecular oxygen was produced within a few seconds after irradiation and maximum O_2 concentration was reached after approximately two minutes. Control experiments showed that

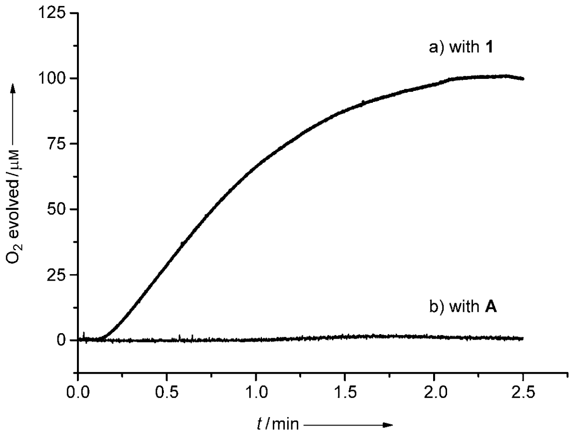

Figure 2. a) O_2 evolution measured with a Clark-type electrode catalyzed by **1** (2.5 μM) under irradiation with visible light (Xe lamp, 500 W, $\lambda > 400$ nm) in the presence of $Na_2S_2O_8$ (10 mM) and $[Ru(bpy)_3Cl_2]$ (0.62 mM) in a phosphate buffer solution (8.3 mM, 1.5 mL, initial pH 7.2); b) **A** (2.5 μM) shows no catalytic activity for light-driven water oxidation under the same conditions.

$[Ru(bpy)_3]^{2+}$, $S_2O_8^{2-}$, and **1** are all necessary to achieve light-driven oxygen evolution. Replacement of **1** with $RuCl_3$ or $[Ru(bpy)_2Cl_2]$ led to no oxygen evolution. As expected, complex **A** showed no activity for light-driven water oxidation under the same conditions (Figure 2b) because water oxidation catalyzed by **A** in the presence of $[Ru(bpy)_3]^{3+}$ as the oxidant is thermodynamically unfavored. These results confirm that light-driven water oxidation is indeed catalyzed by complex **1**.

To further confirm and quantitatively analyze the light-driven oxygen evolution catalyzed by **1** in the presence of $[Ru(bpy)_3]^{2+}$ as the photosensitizer, the dioxygen evolved in the gas phase was detected with GC (see Figure S7 in the Supporting Information). A TN value of approximately 60 and a TOF value of $0.1\,s^{-1}$ were obtained for **1** upon irradiation for 60 minutes. When the more strongly oxidizing sensitizers **P2** ($[Ru(bpy)_2(4,4'\text{-}(CO_2Et)_2\text{-}bpy)]^{2+}$, $E[Ru^{3+/2+}] = 1.4$ V vs. NHE at pH 7.2), and **P3** ($[Ru(bpy)(4,4'\text{-}(CO_2Et)_2\text{-}bpy)_2]^{2+}$, $E[Ru^{3+/2+}] = 1.54$ V vs. NHE at pH 7.2; see structures and properties of **P2** and **P3** the Supporting Information) were used, both the initial rate and the TN value of light-driven water oxidation catalyzed by **1** were increased significantly (see Figure S7 in the Supporting Information). The TN values are 420 and 580 with TOF values of 0.77 and $0.83\,s^{-1}$ in the case of **P2** and **P3** as sensitizers, respectively. These TN values and TOF values for **1** were much higher than those reported previously for **A**.[12b] The quantum yields were found to be 0.7 %, 4.5 %, and 9.7 % in the cases of sensitizers **P1**, **P2**, and **P3**, respectively.

As also found for catalyst **A**,[12b] the pH value of the reaction mixture was greatly decreased (to ca. pH 3) during light-driven water oxidation catalyzed by **1**, and accompanied by CO_2 evolution. As photoinduced ligand oxidation of $[Ru(bpy)_3]^{2+}$ to give CO_2 and protons has been reported previously,[23] the decrease of the pH value during light-driven water oxidation catalyzed by **1** is a result of the proton accumulation by both water oxidation and photoinduced decomposition of the sensitizer.

It was noted that the catalyst was not dead still active when oxygen evolution had ceased. Oxygen evolution could be resumed up irradiation (see Figure S8 in the Supporting Information) when the reaction mixture was neutralized to pH 7.2. This process was repeated three times, while the rate for O_2 evolution became slower after each cycle. Addition of more $Na_2S_2O_8$ could not revive the system. However, addition of more $[Ru(bpy)_3]^{2+}$ gave rise to renewed oxygen evolution upon irradiation. This outcome means that deactivation is mainly due to the decrease of the pH value and the consumption of sensitizer and acceptor. These results clearly show that **1** is very stable and robust for light-driven water oxidation.

In conclusion, we have demonstrated that complex **1** is the most stable and most active ruthenium-based catalyst for water oxidation reported to date. A record high TN value of more than 10000 with a high TOF value of $1.2\,s^{-1}$ has been achieved in the presence of Ce^{IV} as the oxidant at pH 1. Furthermore, the overpotential for water oxidation catalyzed by **1** is sufficiently low so that this reaction can be driven by photogenerated $[Ru(bpy)_3]^{3+}$. This work provides a promising lead for developing a complete artificial photosynthetic system by the use of molecular catalysts. Attempts to immobilize **1** onto electrodes for light-driven water splitting are currently in progress.

Received: July 13, 2010

Keywords: carboxylate ligands · homogeneous catalysis · photocatalysis · ruthenium · water splitting

[1] E. Amouyal, *Sol. Energy Mater. Sol. Cells* **1995**, 38, 249–276.

[2] a) M. Yagi, M. Kaneko, *Chem. Rev.* **2001**, *101*, 21–35; b) C. W. Cady, R. H. Crabtree, G. W. Brudvig, *Coord. Chem. Rev.* **2008**, *252*, 444–455.

[3] L. L. Tinker, N. D. McDaniel, S. Bernhard, *J. Mater. Chem.* **2009**, *19*, 3328–3337.

[4] R. Brimblecombe, G. C. Dismukes, G. F. Swiegers, L. Spiccia, *Dalton Trans.* **2009**, 9374–9384.

[5] J. J. Concepcion, J. W. Jurss, M. K. Brennaman, P. G. Hoertz, A. O. T. Patrocinio, N. Y. M. Iha, J. L. Templeton, T. J. Meyer, *Acc. Chem. Res.* **2009**, *42*, 1954–1965, and references therein.

[6] a) F. Bozoglian, S. Romain, M. Z. Ertem, T. K. Todorova, C. Sens, J. Mola, M. Rodriguez, I. Romero, J. Benet-Buchholz, X. Fontrodona, C. J. Cramer, L. Gagliardi, A. Llobet, *J. Am. Chem. Soc.* **2009**, *131*, 15176–15187; b) X. Sala, I. Romero, M. Rodriguez, L. Escriche, A. Llobet, *Angew. Chem.* **2009**, *121*, 2882–2893; *Angew. Chem. Int. Ed.* **2009**, *48*, 2842–2852; c) I. Romero, M. Rodríguez, C. Sens, J. Mola, M. R. Kollipara, L. Francàs, E. Mas-Marza, L. Escriche, A. Llobet, *Inorg. Chem.* **2008**, *47*, 1824–1834.

[7] a) R. Zong, R. P. Thummel, *J. Am. Chem. Soc.* **2005**, *127*, 12802–12803; b) Z. Deng, H.-W. Tseng, R. Zong, D. Wang, R. Thummel, *Inorg. Chem.* **2008**, *47*, 1835–1848; c) H.-W. Tseng, R. Zong, J. T. Muckerman, R. Thummel, *Inorg. Chem.* **2008**, *47*, 11763–11773.

[8] J. T. Muckerman, D. E. Polyansky, T. Wada, K. Tanaka, E. Fujita, *Inorg. Chem.* **2008**, *47*, 1787–1802.

[9] a) Y. V. Geletii, B. Botar, P. Kögerler, D. A. Hillesheim, D. G. Musaew, C. L. Hill, *Angew. Chem.* **2008**, *120*, 3960 – 3963; *Angew. Chem. Int. Ed.* **2008**, *47*, 3896 – 3899; b) A. Sartorel, M. Carraro, G. Scorrano, R. D. Zorzi, S. Geremia, N. D. McDaniel, S. Bernhard, M. Bonchio, *J. Am. Chem. Soc.* **2008**, *130*, 5006 – 5007.

[10] L. Duan, A. Fischer, Y. Xu, L. Sun, *J. Am. Chem. Soc.* **2009**, *131*, 10397 – 10399.

[11] L. Duan, Y. Xu, P. Zhang, M. Wang, L. Sun, *Inorg. Chem.* **2010**, *49*, 209 – 215.

[12] a) Y. Xu, T. Åkermark, V. Gyollai, D. Zou, L. Eriksson, L. Duan, R. Zhang, B. Åkermark, L. Sun, *Inorg. Chem.* **2009**, *48*, 2717 – 2719; b) Y. Xu, L. Duan, L. Tong, B. Åkermark, L. Sun, *Chem. Commun.* **2010**, *46*, 6506 – 6508.

[13] L. Duan, Y. Xu, M. Gorlov, L. Tong, S. Andersson L. Sun, *Chem. Eur. J.* **2010**, *16*, 4659 – 4668.

[14] J. L. Cape, J. K. Hurst, *J. Am. Chem. Soc.* **2008**, *130*, 827 – 829.

[15] F. P. Rotzinger, S. Munavalli, P. Comte, J. K. Hurst, M. Grätzel, F.-J. Pern, A. J. Frank, *J. Am. Chem. Soc.* **1987**, *109*, 6619 – 6626.

[16] P. Comte, M. K. Nazeeruddin, F. P. Rotzinger, A. J. Frank, M. Grätzel, *J. Mol. Catal.* **1989**, *52*, 63 – 84.

[17] a) Y. V. Geletii, Z. Huang, Y. Hou, D. G. Musaev, T. Lian, C. L. Hill, *J. Am. Chem. Soc.* **2009**, *131*, 7522 – 7523; b) F. Puntoriero, G. L. Ganga, A. Sartorel, M. Carraro, G. Scorrano, M. Bonchio S. Campagna, *Chem. Commun.* **2010**, *46*, 4725 – 4727.

[18] a) M. W. Kanan, Y. Surendranath, D. G. Nocera, *Chem. Soc. Rev.* **2009**, *38*, 109 – 114; b) M. W. Kanan, D. G. Nocera, *Science* **2008**, *321*, 1072 – 1075; c) Q. Yin, J. M. Tan, C. Besson, Y. V. Geletii, D. G. Musaev, A. E. Kuznetsov, Z. Luo, K. I. Hardcastle, C. L. Hill, *Science* **2010**, *328*, 342 – 345.

[19] a) N. D. McDaniel, F. J. Coughlin, L. L. Tinker, S. Bernhard, *J. Am. Chem. Soc.* **2008**, *130*, 210 – 217; b) J. F. Hull, D. Balcells, J. D. Blakemore, C. D. Incarvito, Q. Eisenstein, G. W. Brudvig, R. H. Crabtree, *J. Am. Chem. Soc.* **2009**, *131*, 8730 – 8731.

[20] W. C. Ellis, N. D. McDaniel, S. Bernhard, T. J. Collins, *J. Am. Chem. Soc.* **2010**, *132*, 10990 – 10991.

[21] Structure data of **1**·H_2O: $C_{44}H_{40}ClF_6N_8O_5PRu_2$; $M_r = 1143.4$, crystal dimensions $0.04 \times 0.27 \times 0.43$ mm^3, monoclinic, $P2_1/c$, $a = 14.665(3)$ Å, $b = 12.3240(15)$ Å, $c = 25.983(7)$ Å, $\beta = 90.524(17)°$, $V = 4695.7(17)$ Å, $Z = 4$, $\rho_{calc} = 1.617$ Mg·m^{-3}, $\mu = 0.81$ mm^{-1}, Mo-Kα, $\lambda = 0.71073$ Å, $T = 299$ K, $2\theta_{max} = 51°$, 21412 measured reflections, 7203 independent reflections, $R_{int} = 0.066$, $R = 0.091$ (4906 observed reflections), $wR_2 = 0.226$, S = 1.22, residual electron density 1.17/−1.41. Refinement on F^2 with anisotropic displacement parameters for all non-hydrogen atoms. Hydrogen atoms placed at calculated positions; CCDC 768171 contains the supplementary crystallographic data for this paper. These data can be obtained free of charge from The Cambridge Crystallographic Data Centre via www.ccdc.cam.ac.uk/data_request/cif.

[22] H. A. F. Werner, R. Bauer, *J. Mol. Catal.* **1994**, *88*, 185 – 192.

[23] K. Henbest, P. Douglas, M. S. Garley, A. Mills, *J. Photochem. Photobiol. A* **1994**, *80*, 299 – 305, and references therein.